Jpn. J. Cancer Res. **91**, 837–844, August 2000

TZT-1027, an Antimicrotubule Agent, Attacks Tumor Vasculature and Induces Tumor Cell Death

Masashi Otani,[1,3] Tsugitaka Natsume,[2] Jun-ichi Watanabe,[2] Motohiro Kobayashi,[2] Masanori Murakoshi,[1] Takashi Mikami[1] and Takaharu Nakayama[1]

[1]Safety Research Department and [2]Pharmacological Research Department, Teikoku Hormone Mfg. Co., Ltd., 1604 Shimosakunobe, Takatsu-ku, Kawasaki-shi, Kanagawa 213-8522

TZT-1027, a dolastatin 10 derivative, is an antimicrotubule agent with potent antitumor activity both *in vitro* and *in vivo*. In this study, we performed biochemical and histopathological examinations, and evaluated TZT-1027-induced tumoral vascular collapse and tumor cell death in an advanced tumor model, murine colon 26 adenocarcinoma. In addition, we studied the effects of TZT-1027 on cultured human umbilical vein endothelial cells (HUVEC). Tolerable doses of TZT-1027 induced tumor-selective hemorrhage within 1 h. This hemorrhage occurred mainly in the peripheral area of the tumor mass. Measurements of tumoral hemoglobin content and dye permeation revealed that the hemorrhage occurred firstly and tumor blood flow stopped secondarily. The vascular damage was followed by continuous induction of apoptosis of the tumor cells, tumor tissue necrosis, and tumor regression. In cultured HUVEC, TZT-1027 induced marked cell contraction with membrane blebbing in 30 min. These cell changes were completely inhibited by K252a, a broad-spectrum inhibitor of protein kinases. These effects of TZT-1027 on both tumor vasculature and HUVEC were greater than those of vincristine. In conclusion, TZT-1027 quickly attacked the well-developed vascular system of advanced tumors by a putative protein kinase-dependent mechanism, and then blocked tumor blood flow. Therefore, TZT-1027 has both a conventional antitumor activity and a unique anti-tumoral vascular activity, making it a potentially powerful tool for clinical cancer therapy.

Key words: TZT-1027 — Antimicrotubule agent — Tumoral vascular collapse — Tumor cell death — Advanced tumor

We reported TZT-1027/Sonidotin [N^2-(*N*,*N*-dimethyl-L-valyl)-*N*-[(1*S*,2*R*)-2-methoxy-4-[(2*S*)-2-[(1*R*,2*R*)-1-methoxy-2-methyl-3-oxo-3-[(2-phenylethyl)amino]propyl]-1-pyrrolidinyl]-1-[(*S*)-1-methylpropyl]-4-oxobutyl]-*N*-methyl-L-valinamide], a derivative of dolastatin 10 (a natural product isolated from the marine mollusk *Dolabella auricularia*), to be a potent antitumor agent with little toxicity.[1,2] TZT-1027 is a completely synthetic compound and its large-scale synthesis is feasible. TZT-1027 was reported to be more effective than dolastatin 10 and *Vinca* alkaloids in several experimental mouse tumors and human xenograft models.[2–7] It is currently in clinical trials in Japan.

TZT-1027 inhibits microtubule assembly[2,8] and induces cell cycle arrest and apoptosis *in vitro*.[5–7,9] In addition, our unpublished data show that TZT-1027 also induces hemorrhagic changes in advanced tumor models *in vivo*. Therefore, its antitumor activity *in vivo* was thought to result from induction of tumoral vascular collapse in addition to direct cytotoxicity to tumor cells. Despite several reports that antimicrotubule agents induce tumoral vascular collapse,[10–15] the correlation between the collapse and antitumor activity has not been elucidated. Therefore, in the present study, we examined TZT-1027-induced vascular collapse and tumor cell death in an advanced tumor model, murine colon 26 adenocarcinoma, by means of biochemical and histopathological examinations. We also studied the effects of TZT-1027 on cultured human umbilical vein endothelial cells (HUVEC).

[3] To whom correspondence should be addressed.
E-mail: otani-m@kw.teikoku-hormone.co.jp

MATERIALS AND METHODS

Drugs TZT-1027, a dolastatin 10 derivative, was synthesized in our laboratories.[1] Its chemical structure is shown in Fig. 1. Vincristine (VCR) was purchased from Shionogi Pharmaceutical Co., Ltd. (Osaka). TZT-1027 was dissolved and diluted in 0.05 *M* lactate buffer (pH 4.5) containing 7.3 mg/ml NaCl. VCR was dissolved and diluted in saline.

Animals Female BALB/c and CDF_1 mice were purchased from Charles River Japan Inc. (Kanagawa). Mice were fed a pellet diet (MM-3: Funabashi Farm, Chiba) and given filtered water.

Tumors Colon 26 adenocarcinoma was kindly supplied by the Cancer Chemotherapy Center, Japanese Foundation

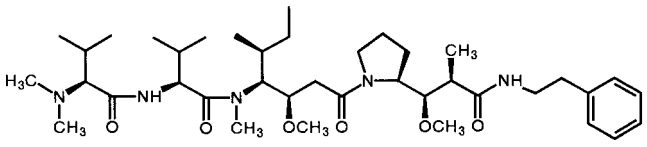

Fig. 1. Chemical structure of TZT-1027.

for Cancer Research, Tokyo. The tumor was maintained in syngeneic BALB/c mice according to the protocol of the National Cancer Institute.[16]

Cell culture HUVEC were purchased from Morinaga Institute of Biological Science (Yokohama). The cells were maintained in "HUVE Cell Culture Medium" (Nissui, Tokyo) in a 5% CO_2 atmosphere at 37°C.

Measurement of tumoral hemoglobin content, dye permeation and tumor weight Tumor fragments (2 mm^3) of colon 26 adenocarcinoma were implanted s.c. in the right flank of female CDF_1 mice, and drugs were administered i.v. in a volume of 10 ml/kg when the tumor had grown to about 1 cm. TZT-1027 and VCR were administered at doses of 0.5, 1.0 and 2.0 mg/kg. These doses were all tolerable in a preclinical evaluation (Q4d×4 treatment),[2] except the 2.0 mg/kg dose of VCR. The mice were killed at various time points (0, 1, 3, 6, 12, 24, 48 and 72 h). One hour beforehand, 0.2% Evans blue was given i.v. at 0.2 ml/head. Under these conditions, Evans blue molecules bind to plasma albumin and behave like albumin.[17] Immediately after death, tumors were isolated and frozen in liquid nitrogen. Tumoral hemoglobin was measured by cyanmethemoglobin methods.[18] Briefly, frozen tumor was crushed into powder and separated into two fractions, each of which was then weighed. One fraction was suspended in 5–10 ml of saline ("Celluent," Sysmex, Kobe). One or 2 drops of hemolytic reagent containing 5.8 g/liter potassium cyanide ("Quicklyser," Sysmex) were added to the tumoral suspension and mixed well. Then, the suspension was filtered on a 5 μm membrane filter (Millipore, Tokyo) and left overnight at room temperature. After the production of cyanmethemoglobin had finished, as recognized from the shape of the light absorption curve, the absorbance (A) at 540 nm (reference at 690 nm) was measured. Hemoglobin content per tumor weight (mg/g) was calculated by comparison with the A value at 540 nm of cyanmethemoglobin standard solution ("Histan," Sysmex). The other tumor fraction was suspended in 1–3 ml of formamide and incubated for 48 h at 60°C to extract the Evans blue.[17] Then, the suspension was filtered on a 5 μm membrane filter and the absorbance at 620 nm (reference at 690 nm) was measured. The absorbance per tumor weight (A/g) was calculated and relative dye permeation in the tumor was expressed as a percentage of the non-treated control.

Analysis of DNA fragmentation Tumor-bearing mice were treated with TZT-1027 (2.0 mg/kg) as described above. The tumors were isolated at 0, 3, 6, 9, 24 or 48 h, frozen in liquid nitrogen and stored at −80°C. DNA was extracted by conventional methods[19] with some modifications. Briefly, frozen tumor was crushed into powder and treated with 50 μg/ml proteinase K (Boehringer Mannheim, Tokyo). Then, DNA was extracted with phenol-chloroform (1:1, vol/vol) and treated with 100 μg/ml RNase (Wako, Osaka). The DNA was extracted with phenol-chloroform again and dissolved in TE buffer (10 mM Tris-HCl pH 8.0, 1 mM EDTA). The DNA (3 μg) was separated electrophoretically on 2% agarose gel at 50 V for 100 min and stained with 0.5 μg/ml ethidium bromide (Wako). The bands of DNA fragments were visualized under UV light and photographed.

Histopathological examination Tumor-bearing mice were treated with TZT-1027 (2.0 mg/kg) as described above. The tumors were isolated at 0, 6, 9, 24 and 48 h and fixed in 0.1 M phosphate-buffered 10% formalin. Then, they were embedded in paraffin, mounted and stained with hematoxylin and eosin (HE).

Microscopy and WST-1 assay of cultured HUVEC HUVEC were plated in human fibronectin-coated 6- or 96-well culture plates (Nippon Becton Dickinson, Tokyo) at about 5000 cells/cm^2 and cultured until confluence. Then, the cells on the 6-well plates were treated with drugs at various concentrations (10^{-10}–10^{-6} g/ml) and observed under a microscope at various time points (0–30 min and 1–24 h). In addition, they were pretreated with 0.5 μM K252a (Nacalai Tesque, Kyoto), a broad-spectrum inhibitor of serine/threonine protein kinases. Fifteen minutes later, the cells were treated with TZT-1027 (10^{-7} g/ml) and again observed. The cells on the 96-well plates were treated with drugs at various concentrations (10^{-12}–10^{-6} g/ml) for 24 h and their viability was evaluated by WST-1 assay ("Cell counting kit," Dojindo Laboratories, Kumamoto). Cell viability was expressed as a percentage of the vehicle-treated control.

Data analysis Quantitative data are given as the mean of five animals. Statistical evaluation was performed by analysis of balance, followed by Dunnett's test or the Dunnett-type t test. $P<0.05$ was considered significant.

RESULTS

Tumoral hemoglobin content TZT-1027 induced marked hemorrhage in tumor tissues within 1 h at all doses tested (0.5, 1.0 and 2.0 mg/kg) and the tumoral hemoglobin content, a parameter of the number of red blood cells in the tumor, increased dose-dependently (Fig. 2). The accumulation of hemoglobin peaked at 6–12 h and then recovered. In addition, based on the hourly increase of hemoglobin content (Fig. 2, a and b), hemorrhage per

hour peaked within 1 h of the treatment, then declined and almost stopped after 6 h. In contrast, VCR induced tumor hemorrhage only at 2.0 mg/kg. However, these changes were no greater than those for TZT-1027 at 0.5 mg/kg.

Permeation of dye in tumor In non-treated and vehicle-treated control mice, marked dye permeation in tumors was evident macroscopically and large amounts of Evans blue, a measure of tumor blood flow and vascular permeability, were detected. TZT-1027 suppressed this permeation in a dose-dependent manner from 3 or 6 h after the treatment (Fig. 3). At 2.0 mg/kg of TZT-1027, the permeation decreased to 24, 22, 29 and 47% at 6, 12, 24 and 48 h, respectively. In contrast, VCR did not affect the dye permeation at 0.5 or 1.0 mg/kg. However, at 2.0 mg/kg, VCR suppressed the dye permeation to 47% in 6 h.

Tumor weight changes Vehicle-treated control tumors grew time-dependently and tumor weight increased to about 2.4 times that at time 0 at 72 h (Fig. 4). TZT-1027 suppressed this growth at both 0.5 and 2.0 mg/kg. At 2.0 mg/kg, TZT-1027 not only suppressed tumor progression, but also decreased tumor weight from 24 to 72 h after the treatment.

Analysis of DNA fragmentation TZT-1027 induces fragmentation of DNA within 3 h and this fragmentation increased time-dependently (Fig. 5). Electrophoretic bands of DNA fragments showed a distinctive ladder pattern, the hallmark of apoptosis. At 24 and 48 h, although the ladder pattern was less clear, the DNA fragmentation was actually increased.

Histopathological findings Non-treated control tumor tissues were filled with tumor parenchyma cells (Fig. 6a). TZT-1027 induced multifocal accumulation and diffuse permeation of red blood cells in the tumors at 6 and 9 h (Fig. 6, b and c). These hemorrhagic changes were more abundant in the peripheral area than in the central area in the tumor mass. In addition, TZT-1027 induced apoptosis-associated nuclear pyknosis in these tumor cells at 6, 9, 24 and 48 h (Fig. 6, b, c, d and e). Furthermore, marked tis-

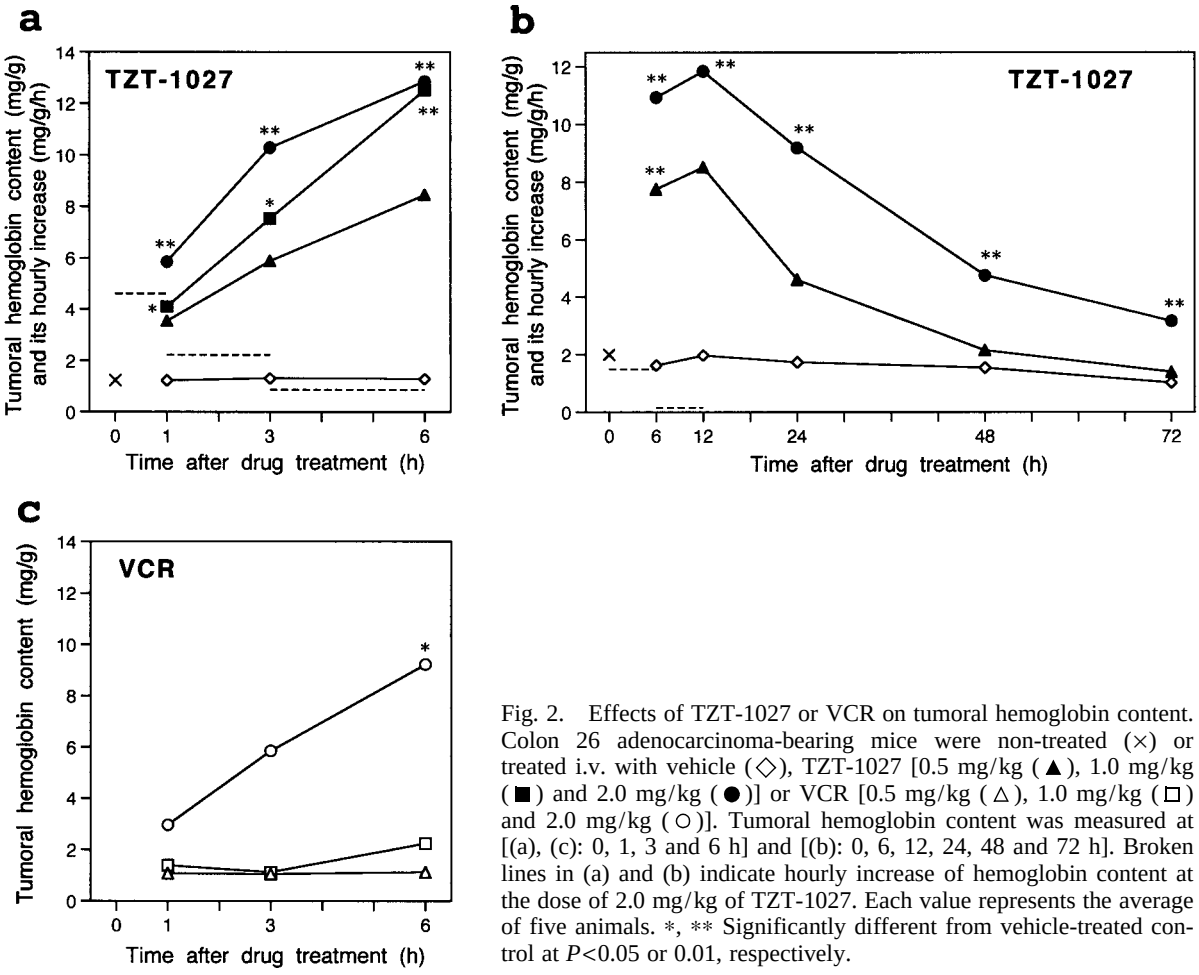

Fig. 2. Effects of TZT-1027 or VCR on tumoral hemoglobin content. Colon 26 adenocarcinoma-bearing mice were non-treated (×) or treated i.v. with vehicle (◇), TZT-1027 [0.5 mg/kg (▲), 1.0 mg/kg (■) and 2.0 mg/kg (●)] or VCR [0.5 mg/kg (△), 1.0 mg/kg (□) and 2.0 mg/kg (○)]. Tumoral hemoglobin content was measured at [(a), (c): 0, 1, 3 and 6 h] and [(b): 0, 6, 12, 24, 48 and 72 h]. Broken lines in (a) and (b) indicate hourly increase of hemoglobin content at the dose of 2.0 mg/kg of TZT-1027. Each value represents the average of five animals. *, ** Significantly different from vehicle-treated control at $P<0.05$ or 0.01, respectively.

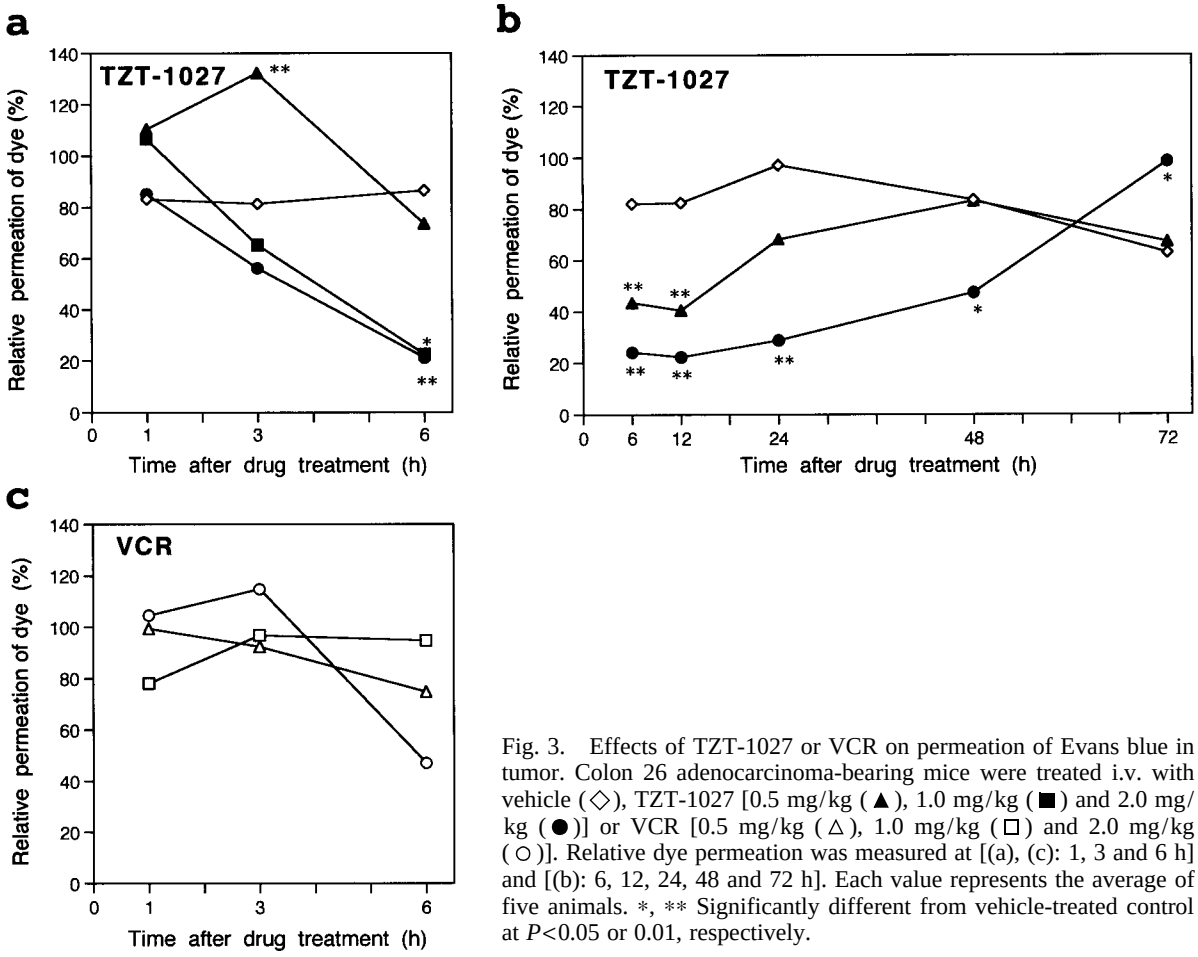

Fig. 3. Effects of TZT-1027 or VCR on permeation of Evans blue in tumor. Colon 26 adenocarcinoma-bearing mice were treated i.v. with vehicle (◇), TZT-1027 [0.5 mg/kg (▲), 1.0 mg/kg (■) and 2.0 mg/kg (●)] or VCR [0.5 mg/kg (△), 1.0 mg/kg (□) and 2.0 mg/kg (○)]. Relative dye permeation was measured at [(a), (c): 1, 3 and 6 h] and [(b): 6, 12, 24, 48 and 72 h]. Each value represents the average of five animals. *, ** Significantly different from vehicle-treated control at $P<0.05$ or 0.01, respectively.

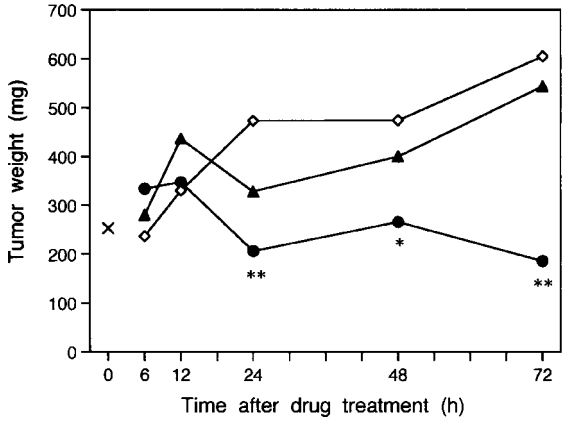

Fig. 4. Tumor weight changes after treatment with TZT-1027. Colon 26 adenocarcinoma-bearing mice were non-treated (×) or treated i.v. with vehicle (◇) or TZT-1027 [0.5 mg/kg (▲) and 2.0 mg/kg (●)]. Tumor weights were measured at 0, 6, 12, 24, 48 and 72 h. Each value represents the average of five animals. *, ** Significantly different from vehicle-treated control at $P<0.05$ or 0.01, respectively.

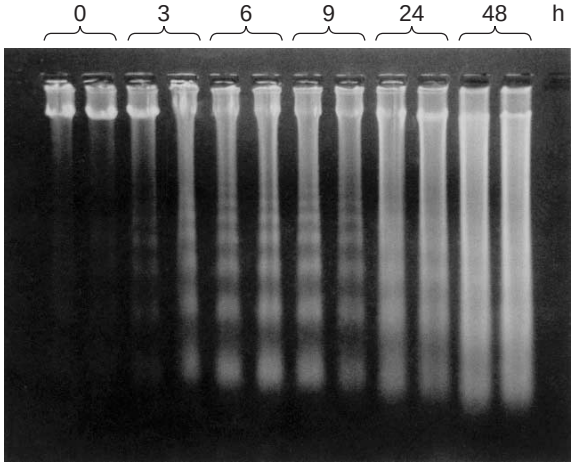

Fig. 5. Tumor DNA fragmentation induced by TZT-1027. Colon 26 adenocarcinoma-bearing mice were treated i.v. with TZT-1027 (2.0 mg/kg). Tumor DNA was extracted at 0, 3, 6, 9, 24 and 48 h and separated electrophoretically. Two animals were used at each time point.

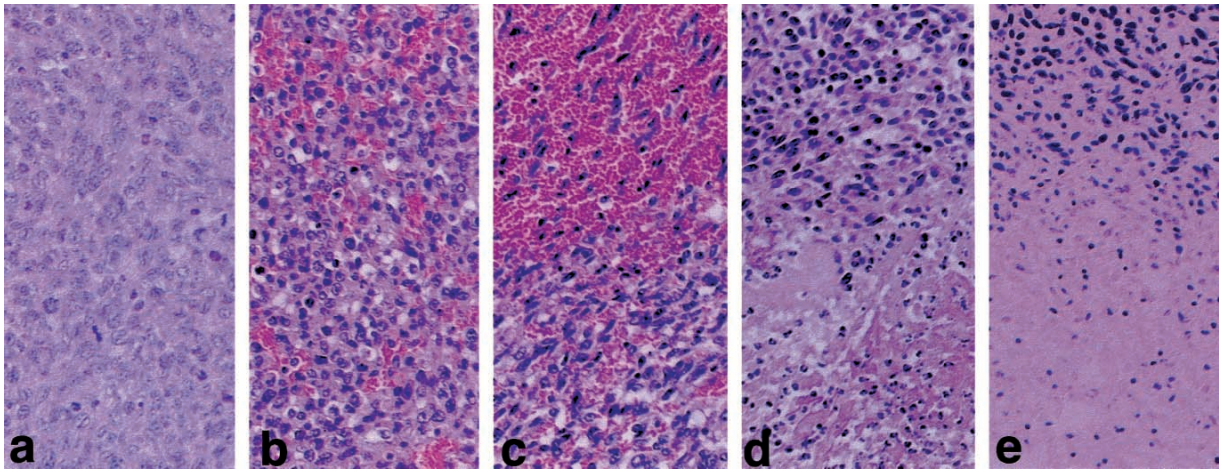

Fig. 6. Histopathological findings in colon 26 adenocarcinoma (HE). Colon 26 adenocarcinoma-bearing mice were treated i.v. with TZT-1027 (2.0 mg/kg). (a) 0 h, (b) 6 h, (c) 9 h, (d) 24 h, (e) 48 h. Tops of the photos correspond to the peripheral area and the bottoms correspond to the central area of the tumor mass. (Original magnifications ×200).

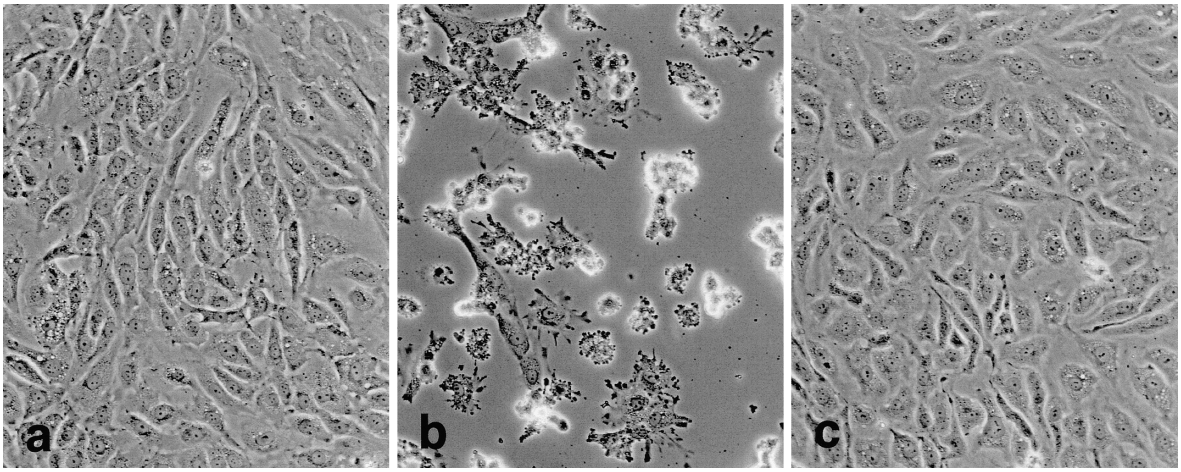

Fig. 7. Microscopical observations in cultured HUVEC. HUVEC were cultured to confluency and treated with TZT-1027 for 30 min. (a) No treatment, (b) TZT-1027 (10^{-7} g/ml), (c) TZT-1027 (10^{-7} g/ml) after pretreatment with 0.5 μM K252a.

sue necrosis was co-observed mainly in the central area at 24 and 48 h (Fig. 6, d and e).

Microscopy and WST-1 assay of cultured HUVEC

Microscopy revealed that TZT-1027 quickly induced cell changes, generally cell contraction without any changes of nuclei, at 10^{-9} g/ml or more. These changes were intensified concentration-dependently and reached a maximum 30 min to 1 h after the treatment. At concentrations of 10^{-7} g/ml and above, marked cell contraction with membrane blebbing was observed in most of the cells and a number of the cells became detached from the culture surface (Fig. 7b). These cell changes induced by TZT-1027 were completely inhibited by pretreatment with 0.5 μM K252a (Fig. 7c). VCR induced similar changes at 10-fold higher doses of TZT-1027. In WST-1 assay, cell viability was reduced to 50–60% of the control at concentrations of 10^{-9} g/ml and above, 24 h after the treatment with TZT-1027 (Fig. 8). VCR had a similar effect at 10^{-8} g/ml and above.

DISCUSSION

TZT-1027 induced marked tumor hemorrhage. The hemorrhage was abundant in the peripheral area in the tumor mass. This change could be easily detected, not

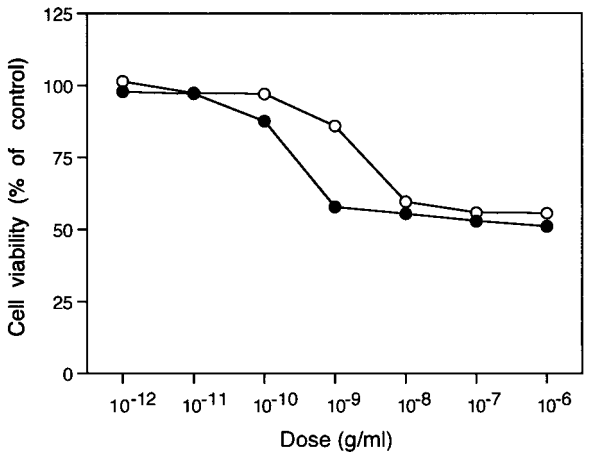

Fig. 8. WST-1 assay in cultured HUVEC. HUVEC were cultured to confluency and treated with TZT-1027 (●) or VCR (○) at various doses (10^{-12}, 10^{-11}, 10^{-10}, 10^{-9}, 10^{-8}, 10^{-7} and 10^{-6} g/ml) for 24 h. Then, cell viability was measured by WST-1 assay. Each value represents the average of three individual experiments.

only by histopathological analysis, but also grossly. However, no hemorrhagic changes were grossly observed in normal tissues and organs. Therefore, TZT-1027 appears to selectively attack the tumor vasculature. The hemorrhage resulted in an increase of the tumoral hemoglobin content. The hemorrhage per hour peaked within 1 h of the treatment, then declined and almost stopped after 6 h. These changes were followed by a decrease of dye permeation in the tumor. This shows that the marked suppression of tumor blood flow and/or vascular permeability persisted from 6 to 48 h. Therefore, it is thought that multiple vascular damage including hemorrhage occurred in the peripheral area of the tumor mass firstly, and the blood flow through this area to the central area was stopped secondarily.

Enhanced vascular permeability has been reported in many solid tumors. It is thought to result from tumor secretion of vascular endothelial growth factor (VEGF), etc.[20, 21] In the present study, circulating dye markedly permeated into control tumors, that is, blood flow and vascular permeability were highly activated. When vascular collapse occurs, two anti-tumor mechanisms are expected to operate. The first is that exclusion of the drug is suppressed and a high drug concentration is maintained in the tumor, resulting in continuous cytotoxicity including induction of apoptosis of the tumor cells. The second is that ischemia occurs in the central area of the tumor mass, resulting in tissue necrosis. In fact, DNA fragmentation and histopathological findings revealed that tumor cell apoptosis persisted from 3 to at least 48 h. In addition, marked tissue necrosis occurred mainly in the central area of the tumor mass at 24 and 48 h. This cell death was directly related to tumor regression as shown by the decrease in tumor weight.

Anti-tumoral vascular activity, as well as antimitotic activity, is thought to be a common feature of antimicrotubule agents.[10–15] However, the potency of the activity differs among drugs. In the present study, TZT-1027 induced hemorrhage at all tested doses (0.5, 1.0 and 2.0 mg/kg) in a dose-dependent manner. In contrast, VCR induced hemorrhage only at 2.0 mg/kg, and was no more potent than TZT-1027 at 0.5 mg/kg. In addition, 0.5, 1.0 and 2.0 mg/kg of TZT-1027 were dose-dependently effective against colon 26 adenocarcinoma in the preclinical evaluation (Q4d×4 treatment),[2] with treated/control tumor volume ratio (T/C) values of 59%, 11% and 5%, respectively. In contrast, T/C values of VCR at 0.5 and 1.0 mg/kg were 88% and 62%, respectively, and that at 2.0 mg/kg could not be determined because of high toxicity. Therefore, TZT-1027 has a more potent anti-tumoral vascular activity than VCR, in agreement with the preclinical evaluation. AC-7700, a combretastatin A-4 derivative, is a potent anti-tumoral vascular agent with little antimitotic activity *in vivo*.[15] At the maximal tolerable dose, AC-7700 suppressed permeation of Evans blue in colon 26 adenocarcinoma to about 25% of the non-treated control value at 6 h, with a recovery to more than 60% at 24 h.[15] In contrast, at 2.0 mg/kg, a tolerable dose, TZT-1027 suppressed the permeation of dye to 24%, 22%, 29% and 47% in 6, 12, 24 and 48 h, respectively, in our study. Therefore, TZT-1027 is thought to have stronger anti-tumoral vascular activity than AC-7700, as well as VCR.

The mechanism of the induction of tumor-selective vascular collapse by antimicrotubule agents is unclear. It may be due to fragility of the tumor vasculature caused by a lack of pelicytes or immature basement membrane.[22–24] Judging from the rapid time-course, the vascular collapse does not result from inhibition of endothelial mitosis or migration combined with angiogenesis. This conclusion is consistent with the reports of Dark *et al.*[13] and Hori *et al.*[14] Hori *et al.* speculated that the vascular collapse occurred as a result of contraction of host arteries rather than direct changes to the tumor vasculature. However, in the case of our present study, the quickly induced tumor hemorrhage can not be explained in terms of such an indirect mechanism. TZT-1027 is thought to directly attack the tumor vasculature. In cultured HUVEC, TZT-1027 induced marked cell contraction with membrane blebbing. These cell changes reached a maximum in 30 min to 1 h, and this time-course corresponded well to the hemorrhagic time-course *in vivo*: tumor hemorrhage peaked at 1 h after treatment with TZT-1027. Furthermore, the *in vitro* effects of TZT-1027 were about 10 times greater than those of VCR, and this also corresponded well to the results *in vivo*. In addition, cell shape changes in endothelium were

reported, along with hemorrhage, edema and infarction.[25–27] Therefore, it was suggested that cell changes observed in cultured HUVEC result in tumoral vascular collapse *in vivo*. Because the cell changes in HUVEC were completely inhibited by K252a, TZT-1027-induced tumoral vascular collapse is thought to involve a protein kinase-dependent mechanism.

Since angiogenesis is essential for tumor progression,[28–30] tumor angiogenesis has become a chemotherapeutic target. However, most antiangiogenic agents are not expected to regress advanced tumors, although they may stop tumor growth. In contrast, TZT-1027 is expected to cause massive regression because of its ability to directly induce apoptosis and to attack the well-developed vascular system of advanced tumors. Therefore, TZT-1027 has both conventional antitumor activity and a characteristic tumor-selective antivascular activity, making it a potentially powerful tool for clinical cancer therapy.

ACKNOWLEDGMENTS

We thank M. Isobe for his valuable advice and N. Fujio for her excellent technical assistance.

(Received February 17, 2000/Revised May 17, 2000/Accepted June 2, 2000)

REFERENCES

1) Miyazaki, K., Kobayashi, M., Natsume, T., Gondo, M., Mikami, T., Sakakibara, K. and Tsukagoshi, S. Synthesis and antitumor activity of novel dolastatin 10 analogs. *Chem. Pharm. Bull.*, **43**, 1706–1718 (1995).
2) Kobayashi, M., Natsume, T., Tamaoki, S., Watanabe, J., Asano, H., Mikami, T., Miyasaka, K., Miyazaki, K., Gondo, M., Sakakibara, K. and Tsukagoshi, S. Antitumor activity of TZT-1027, a novel dolastatin 10 derivative. *Jpn. J. Cancer Res.*, **88**, 316–327 (1997).
3) Mohammad, R. M., Pettit, G. R., Almatchy, V. P., Wall, N., Varterasian, M. and Al-Katib, A. Synergistic interaction of selected marine animal anticancer drugs against human diffuse large cell lymphoma. *Anticancer Drugs*, **9**, 149–156 (1998).
4) Mohammad, R. M., Al-Katib, A., Pettit, G. R., Vaitkevicius, V. K., Joshi, U., Adsay, V., Majumdar, A. P. and Sarkar, F. H. An orthotropic model of human pancreatic cancer in severe combined immunodeficient mice: potential application for preclinical studies. *Clin. Cancer Res.*, **4**, 887–894 (1998).
5) Mohammad, R. M., Varterasian, M. L., Almatchy, V. P., Hannoudi, G. N., Pettit, G. R. and Al-Katib, A. Successful treatment of human chronic lymphocytic leukemia xenografts with combination biological agents auristatin PE and bryostatin 1. *Clin. Cancer Res.*, **4**, 1337–1343 (1998).
6) Li, Y., Singh, B., Ali, N. and Sarkar, F. H. Induction of growth inhibition and apoptosis in pancreatic cancer cells by auristatin-PE and gemcitabine. *Int. J. Mol. Med.*, **3**, 647–653 (1999).
7) Mohammad, R. M., Limvarapuss, C., Wall, N. R., Hamdy, N., Beck, F. W., Pettit, G. R. and Al-Katib, A. A new tubulin polymerization inhibitor, auristatin PE, induces tumor regression in a human Waldenstorm's macroglobulinemia xenograft model. *Int. J. Oncol.*, **15**, 367–372 (1999).
8) Natsume, T., Watanabe, J., Tamaoki, S., Fujio, N., Miyasaka, K. and Kobayashi, M. Characterization of the interaction of TZT-1027, a potent antitumor agent, with tubulin. *Jpn. J. Cancer Res.*, **91** (2000), in press.
9) Watanabe, J., Natsume, T., Fujio, N., Miyasaka, K. and Kobayashi, M. Induction of apoptosis in human cancer cells by TZT-1027, an antimicrotubule agent. *Apoptosis*, **5** (2000), in press.
10) Hill, S. A., Lonergan, S. J., Denekamp, J. and Chaplin, D. J. *Vinca* alkaloids: anti-vascular effects in a murine tumour. *Eur. J. Cancer*, **29A**, 1320–1324 (1993).
11) Baguley, B. C., Holdaway, K. M., Thomsen, L. L., Zhuang, L. and Zwi, L. J. Inhibition of growth of colon 38 adenocarcinoma by vinblastine and colchicine: evidence for a vascular mechanism. *Eur. J. Cancer*, **27**, 482–487 (1991).
12) Chaplin, D. J., Pettit, G. R., Parkins, C. S. and Hill, S. A. Antivascular approaches to solid tumour therapy: evaluation of tubulin binding agents. *Br. J. Cancer Suppl.*, **27**, S86–S88 (1996).
13) Dark, G. G., Hill, S. A., Prise, V. E., Tozer, G. M., Pettit, G. R. and Chaplin, D. J. Combretastatin A-4, an agent that displays potent and selective toxicity toward tumor vasculature. *Cancer Res.*, **57**, 1829–1834 (1997).
14) Hori, K., Saito, S., Nihei, Y., Suzuki, M. and Sato, Y. Antitumor effects due to irreversible stoppage of tumor tissue blood flow: evaluation of a novel combretastatin A-4 derivative, AC7700. *Jpn. J. Cancer Res.*, **90**, 1026–1038 (1999).
15) Nihei, Y., Suzuki, M., Okano, A., Tsuji, T., Akiyama, Y., Tsuruo, T., Saito, S., Hori, K. and Sato, Y. Evaluation of antivascular and antimitotic effects of tubulin binding agents in solid tumor therapy. *Jpn. J. Cancer Res.*, **90**, 1387–1395 (1999).
16) Geran, R. I., Greenberg, N. H., Macdonald, M. M., Schumacher, A. M. and Abott, B. J. Protocols for screening chemical agents and natural products against animal tumor and other biochemical systems (3rd ed.). *Cancer Chemother. Rep. [3]*, **3**, 1–103 (1972).
17) Matsumura, Y. and Maeda, H. A new concept for macromolecular therapeutics in cancer chemotherapy: mechanism of tumoritropic accumulation of proteins and the antitumor agent smancs. *Cancer Res.*, **46**, 6387–6392 (1986).
18) Crosby, W. H., Munn, J. I. and Furth, F. W. Standardizing a method for clinical hemoglobinometry. *US Armed Forces*

Med. J., **5**, 693–703 (1954).
19) Compton, M. M. and Cidlowsky, J. A. Rapid *in vivo* effects of glucocorticoids on the integrity of rat lymphocyte genomic deoxyribonucleic acid. *Endocrinology*, **118**, 38–45 (1986).
20) Senger, D. R., Van de Water, L., Brown, L. F., Nagy, J. A., Yeo, T. K., Berse, B., Jackman, R. W., Dvorak, A. M. and Dvorak, H. F. Vascular permeability factor (VPF, VEGF) in tumor biology. *Cancer Metastasis Rev.*, **12**, 303–324 (1993).
21) Dvorak, H. F., Brown, L. F., Detmar, M. and Dvorak, A. M. Vascular permeability factor/vascular endothelial growth factor, microvascular hyperpermeability, and angiogenesis. *Am. J. Pathol.*, **146**, 1029–1039 (1995).
22) Blood, C. H. and Zetter, B. R. Tumor interactions with the vasculature: angiogenesis and tumor metastasis. *Biochim. Biophys. Acta*, **1032**, 89–118 (1990).
23) Dvorak, H. F., Nagy, J. A. and Dvorak, A. M. Structure of solid tumors and their vasculature: implications for therapy with monoclonal antibodies. *Cancer Cells*, **3**, 77–85 (1991).
24) Molema, G., de Leij, L. F. and Meijer, D. K. Tumor vascular endothelium: barrier or target in tumor directed drug delivery and immunotherapy. *Pharm. Res.*, **14**, 2–10 (1997).
25) Gores, G. J., Herman, B. and Lemasters, J. J. Plasma membrane bleb formation and rupture: common feature of hepatocellular injury. *Hepatology*, **11**, 690–698 (1990).
26) Becker, L. C. and Ambrosio, G. Myocardial consequences of reperfusion. *Prog. Cardiovasc. Dis.*, **30**, 23–44 (1987).
27) Johnson, K. J., Wilson, B. S., Till, G. O. and Ward, P. A. Acute lung injury in rat caused by immunogloblin A immune complexes. *J. Clin. Invest.*, **74**, 358–369 (1984).
28) Folkman, J. Tumor angiogenesis: therapeutic implications. *N. Engl. J. Med.*, **285**, 1182–1186 (1971).
29) Folkman, J. The role of angiogenesis in tumor growth. *Semin. Cancer Biol.*, **3**, 65–71 (1992).
30) Folkman, J. and Ingber, D. Inhibition of angiogenesis. *Semin. Cancer Biol.*, **3**, 89–96 (1992).